Time-Resolved Optical Second Harmonic Generation Measurements of Picosecond Band Flattening Processes at Single Crystal TiO_2 Electrodes

Juliette M. Lantz and Robert M. Corn*

Department of Chemistry, University of Wisconsin—Madison, 1101 University Ave., Madison, Wisconsin 53706

Received: July 7, 1994[⊗]

Time-resolved optical second harmonic generation (SHG) is used to probe the variations in the surface electrostatic fields that occur under pulsed UV (supra-bandgap) illumination at a n-TiO_2(001) electrode. The interfacial SHG is dominated by the electric field-induced second harmonic response from the first 20 nm of the semiconductor surface; this large SHG signal decreases sharply under UV illumination due to the creation of a steady-state photogenerated hole population at the interface. An additional transient drop in SHG intensity is observed when the pump and probe beams are overlapped temporally on the TiO_2 surface. The time scale for this additional band flattening is determined by the finite time required for photogenerated holes to migrate to the interface under the influence of the surface electrostatic fields. An average transit time of 25 ps that is independent of applied potential or solution composition is observed; this corresponds to a hole drift velocity of 4.0×10^4 cm s^{-1} at the TiO_2 surface. The SHG intensity is found to return to its steady-state level in 3−4 ns due to the removal of the excess holes at the surface by electrochemical charge transfer and surface recombination processes.

Ultrafast processes at semiconductor electrodes have been studied extensively in an effort to elucidate the complex surface reaction kinetics and electron transport dynamics that control the overall reactivity of this electrode/electrolyte interface.[1,2] Phenomena such as charge carrier transport, carrier thermalization, interfacial charge transfer, surface recombination, and surface charge trapping can all contribute to the effectiveness (or ineffectiveness) of a particular semiconductor in a photocatalytic or energy generation device.[1-5] The TiO_2/H_2O interface is a semiconductor/electrolyte interface that has been employed in a variety of technologically important applications[4] and has been the subject of numerous time-resolved experiments including the study of electron injection into the conduction band,[6] hot versus thermalized charge transfer and recombination lifetimes,[7] inverted charge transfer,[8] and dye sensitization.[9] However, several crucial questions concerning the mechanisms and time scales of charge carrier transport and interfacial electron transfer at this interface still remain unanswered.[1,2]

The very fast time scales for processes such as charge generation, charge transport, and charge transfer at semiconductor surfaces[1] make them extremely difficult or even impossible to monitor with standard electrochemical methods.[10] Therefore, optical techniques capable of nearly instantaneous response times such as transient grating measurements,[6,7] photoluminescence,[11,12] time-resolved fluorescence,[9] reflective electrooptic sampling,[13] resonance Raman,[14] and transient absorption spectroscopy[8,15] have been employed. In a previous paper, we demonstrated that the surface-sensitive technique of optical second harmonic generation (SHG)[16-20] can be used as a probe of the dc electric fields and band bending at the surface of TiO_2 electrodes *in situ*.[21] The electrostatic fields at semiconductor interfaces have also been monitored with SHG at Si[22,23] and GaAs surfaces.[24] In a second paper, we recently examined steady-state charge transfer and charge accumulation processes at TiO_2 electrodes during UV (supra-bandgap) excitation.[25] In this Letter, we extend our SHG studies of the TiO_2/electrolyte interface to the observation of ultrafast band-flattening events that result from hole transport, charge transfer, and surface recombination processes on a picosecond time scale.

The *in situ* SHG experiments were performed on an n-doped single crystal TiO_2(001) electrode ($N_d = 10^{15}$ cm^{-3}) prepared in a manner described previously.[21] Electrochemical measurements on the n-TiO_2 sample were obtained with a Princeton Applied Research 173/175 potentiostat in a three-electrode Teflon cell using a Pt counter electrode and a NaCl saturated calomel reference electrode (SSCE). Solutions were prepared from Millipore-filtered water and contained 0.1 M $NaClO_4$ (Fluka) as the supporting electrolyte; the pH of these solutions was controlled by the addition of $HClO_4$ (GFS Chemicals) or NaOH (Fluka). When indicated, 10 mM Na_2HPO_4 (Fluka) was used as a buffer. The SHG measurements on the n-TiO_2 electrode were obtained using a probe beam that was the p-polarized 584 nm output of a pulsed dye laser (4 MHz repetition rate, 2 ps pulse width, 30 nJ pulse energy) focused to a 150 μm spot on the electrode surface with an incident angle of 60° from the surface normal. Both the s-polarized and p-polarized second harmonic light at 292 nm generated in reflection from the surface were detected with a cooled PMT and gated photon counting electronics.[26] Changes in the magnitude of the SHG from the electrode surface were produced by the supra-bandgap excitation of the semiconductor surface with a UV pump beam that was the doubled output at 320 nm from a 640 nm pulsed dye laser identical to that used for the SHG probe beam (4 MHz repetition rate, 2 ps pulse width, 0.8 nJ/pulse in the UV, 250 μm spot size, CW power density of 6 W cm^{-2}). The changes in the surface SHG upon UV illumination were observed only when the pump and probe beams were overlapped spatially on the TiO_2 electrode. As described in a previous paper, the steady-state response to the UV illumination was obtained by temporally separating the pump and probe pulses by >25 ns.[25] In this Letter, the time-resolved transient SHG response of the TiO_2 electrode surface was obtained by using a delay line to temporally overlap the pump and probe pulses. Only changes on time scales less than 250 ns could be observed, as limited by the 4 MHz repetition rate of the laser. The temporal resolution in these experiments is 3.5 ps as determined from a two-beam SHG autocorrelation experiment of the 584 nm probe laser and a sum frequency generation cross-correlation experiment of the 584 and 640 nm laser beams using

[⊗] Abstract published in *Advance ACS Abstracts*, September 1, 1994.

0022-3654/94/2098-9387$04.50/0

a z-cut quartz reference surface. A more detailed description of the time-resolved SHG experimental apparatus is given elsewhere.[27]

The surface SHG from an n-doped TiO_2 electrode in the absence of UV illumination is plotted as a function of applied potential in Figure 1a (filled circles) along with the corresponding potential-dependent current response in Figure 1b (filled squares). As reported previously,[21,25] a large SHG response was observed from the electrode in the depletion region due to the electric field-induced second harmonic (EFISH) response of the polarized TiO_2 lattice at the semiconductor surface. An n-type semiconductor electrode that is held at potentials positive of the flatband potential (V_{fb}) has a space charge layer whose total charge (q_{sc}) can be described in the Mott–Schottky approximation by eq 1[28–30]

$$q_{sc} = (2\epsilon_0 \epsilon e N_d)^{1/2} \Delta V_{sc}^{1/2} \quad (1)$$

where ϵ is the dielectric constant of TiO_2 (=173 parallel to the c axis of the crystal[31]), N_d is the doping density of the semiconductor, and ΔV_{sc} ($=V - V_{fb}$) is the band bending or the total drop in potential from the surface to the bulk of the electrode. The width of the space charge layer also varies with ΔV_{sc} and N_d and is approximately 4 μm at 1 V of band bending for an n-TiO_2 electrode with $N_d = 10^{15}$ dopants cm^{-3}.[31] The excess charge density in this space charge layer creates a large electrostatic field that polarizes the TiO_2 lattice near the electrode surface and effectively breaks the centrosymmetry of the crystal, resulting in a large EFISH response. This EFISH response dominates the SHG from the interface,[21,25] and the SHG intensity is therefore proportional to $|\chi^{(3)}:E_{dc}|^2$ where $\chi^{(3)}$ is the third-order nonlinear hyperpolarizability of the TiO_2 crystal.[16,24,32–36]

While the electrostatic fields at the TiO_2 surface are present throughout the space charge layer, the second harmonic light at 292 nm is energetically above the bandgap for TiO_2 (3.02 eV or 410 nm) so that only the EFISH response within an escape depth from the electrode surface contributes to the second harmonic intensity observed in reflection. Using an absorption coefficient of 8×10^5 cm^{-1},[31] this escape depth is estimated to be approximately 20 nm. Hence, through the EFISH mechanism, the SHG measurements probe the electrostatic fields in the first 20 nm of the TiO_2 at the semiconductor electrode/electrolyte interface. The magnitude of E_{dc} at the surface of the electrode can be obtained by combining Gauss' law with eq 1:[28,29]

$$E_{dc}|_{x=0} = \left(\frac{2eN_d\Delta V_{sc}}{\epsilon_0 \epsilon}\right)^{1/2} \quad (2)$$

Using eq 2, we calculate that E_{dc} at the electrode surface varies from 0 at V_{fb} to 5.6 kV cm^{-1} at the maximum applied potential of 1.0 V shown in Figure 1a. Since the SHG intensity varies as the square of the dc electric fields, eq 2 predicts that the SHG signal will be linearly proportional to the band bending, ΔV_{sc}, with a minimum at $\Delta V_{sc} = 0$, the flatband potential (V_{fb}).[21] In Figure 1a, the SHG intensity was observed to increase linearly with applied potential in the depletion region as expected, and a V_{fb} of −0.5 V versus SSCE was ascertained from this optical measurement.

Also plotted in Figure 1 are the steady-state SHG (open circles) and current (open squares) from the TiO_2 electrode as a function of potential during the illumination of the surface with UV light at 320 nm. As described previously, a large decrease was observed in the SHG intensity when UV light was coincident on the TiO_2 surface.[25] Illuminating the TiO_2 semiconductor electrode with light at 320 nm creates mobile charge carriers in the form of electron–hole (e–h) pairs. Again, the strong absorption of this supra-bandgap pump light by the

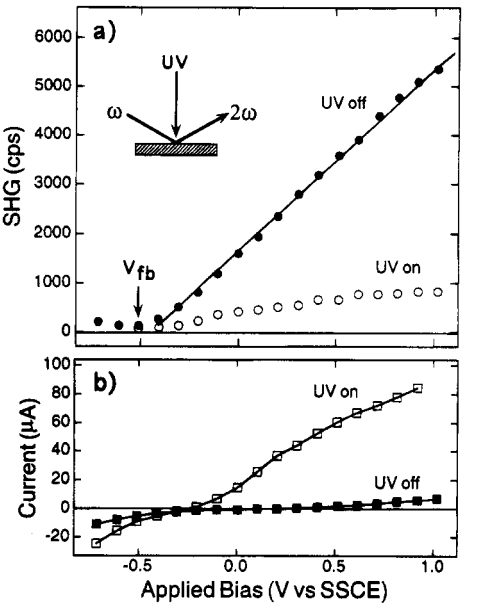

Figure 1. (a) SHG signal as a function of applied potential from an n-TiO_2 electrode with (open circles) and without (filled circles) UV light coincident on the TiO_2 surface in 0.1 M $NaClO_4$ + 10 mM Na_2HPO_4 at pH = 2. $N_d = 10^{15}$ cm^{-3}. In the UV-off case, the SHG is fit with a straight line whose intercept is the flatband potential (V_{fb} = −0.5 V) for this electrode/electrolyte interface. In the UV-on case, the diminished SHG intensity is indicative of the band flattening processes occurring at the TiO_2 surface. (b) Current versus applied potential from the TiO_2 electrode with (open squares) and without (filled squares) UV excitation.

TiO_2 crystal dictates that the e–h pairs will only be created in the first ≈20 nm of the space charge region. When the electrode is held at potentials positive of V_{fb}, the e–h pairs are separated under the influence of the dc electric fields, with the holes being driven to the electrode/electrolyte interface and the electrons into the bulk of the TiO_2. An oxidation current arises from the interfacial charge transfer of the photogenerated holes at the TiO_2/electrolyte interface. Because there is a finite interfacial electron transfer rate, a steady-state concentration of photogenerated holes accumulates at the TiO_2 surface. This steady-state hole concentration at the surface reduces the amount of charge present in the space charge region (q_{sc}), which in turn lowers the dc electric fields and consequently the SHG signal. Concomitant with the decrease in the electric fields, the band bending ΔV_{sc} decreases to a new steady-state value, $\Delta V'_{sc}$; this decrease in the band bending is described as band flattening.[25] From the magnitude of the SHG during UV illumination in Figure 1a, the effective band bending under illumination, $\Delta V'_{sc}$, was found to vary in magnitude from 0 to 0.3 V over the potential range shown in Figure 1a.

In conjunction with the steady-state band-flattening process, an additional transient band flattening was also observed and is plotted in Figure 2. In this series of time-resolved SHG experiments, the difference in arrival times of the picosecond pump and probe pulses on the TiO_2 electrode surface was adjusted with an optical delay line; the experimental geometry is depicted schematically in the inset of Figure 2. The SHG from the electrode surface decreased from its steady-state value when the probe beam was delayed with respect to the pump beam by greater than ≈50 ps and less than ≈5 ns. The exact time scale for the transient drop in SHG intensity is indicative of the time required for the holes generated in the first 20 nm of the space charge region to migrate to the surface and is examined in further detail below. The magnitude of this additional drop in SHG intensity varied linearly with UV pump power over the range of power densities employed in the experiments.

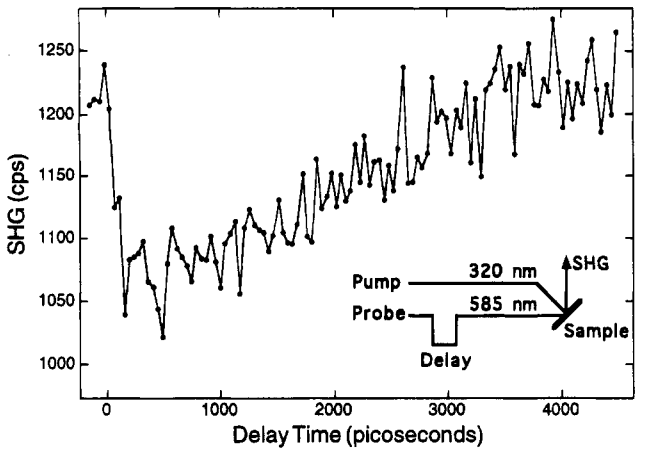

Figure 2. Time-resolved SHG measurements of the transient band flattening that occurs at the TiO_2 electrode surface under supra−bandgap excitation at 320 nm. The inset displays the geometry and optical delay configuration of the picosecond time-resolved pump−probe experiment. A drop in the SHG intensity is observed when the probe beam is delayed from the pump beam by >50 ps and <5 ns; this drop is attributed to a transient excess of photogenerated holes at the interface which effectively decreases the surface electrostatic fields. The SHG signal returns to its steady-state band-flattened level in 3−4 ns, as the excess holes at the surface are removed by either electrochemical or surface recombination processes. The electrode is held at a potential of 0.3 V in the same solution as in Figure 1.

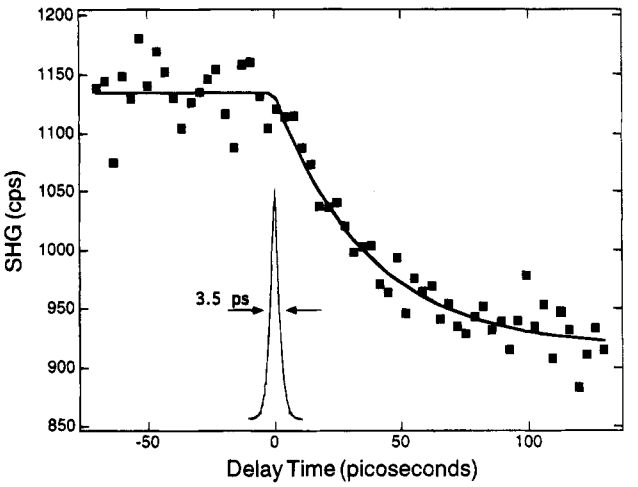

Figure 3. Ultrafast transient band flattening as measured by high-resolution picosecond time-resolved SHG (filled squares). This transient drop is attributed to the finite time required for the transport of the photogenerated holes from their point of origin to the electrode/solution interface. The data are fit with an exponential decay function (solid line) yielding a time constant, τ, of 36 ps for this particular location on the surface. The sharp peak shown in the figure with a fwhm of 3.5 ps is the instrument response function obtained from an autocorrelation SHG experiment performed with the 584 nm probe beam. The electrode is held at a potential of 0.0 V in the solution described in Figure 1.

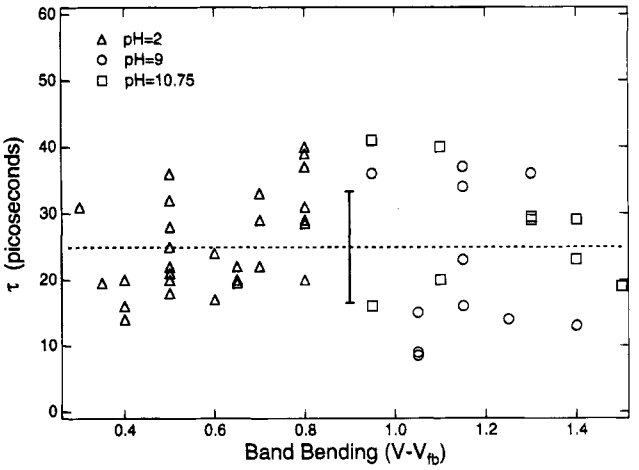

Figure 4. Picosecond hole transport time, τ, as a function of band bending (ΔV_{sc}) at the TiO_2 electrode surface. Data were obtained at three different pH values as shown in the figure legend. The band bending is equal to $V - V_{fb}$, where V_{fb} was determined for each solution optically via SHG measurements as in Figure 1. All solutions contained 0.1 M $NaClO_4$. The average value of τ is 25 ps, which is indicated by the horizontal dashed line. The standard deviation for these measurements is 8 ps and is attributed primarily to surface inhomogeneities; the error bar shown has a height of $\pm\ \sigma$.

While the transient drop in the surface SHG from the TiO_2 electrode occurred on a picosecond time scale, the return of the surface SHG to its original steady-state value occurred as the probe beam was delayed with respect to the pump beam on the order of 3−4 ns (Figure 2). This longer time scale for the recovery of the steady-state interfacial electrostatic fields is attributed to the removal of the photogenerated holes at the surface through either electrochemical consumption or surface recombination and does not vary significantly (±1 ns) with applied potential. The time scales that have been reported previously for these two interfacial processes vary from milliseconds to picoseconds, representing the difficulties in measuring the various charge transfer events that occur at this interface.[1,37] Miller and co-workers[7] have observed interfacial charge transfer and surface recombination at n-TiO_2 electrodes optically with transient grating experiments; they report time scales of 500 ps and 5 ns for the two processes, respectively. Transient grating methods have also been employed by Nakabayashi et al.[6] to optically monitor the photoelectrochemical oxidation of propanol at n-TiO_2 electrodes on a time scale of 400 ns. On TiO_2 colloids, interfacial charge transfer processes have been observed with time-resolved fluorescence and absorption measurements on the time scale of 0.5−500 ns.[8,9] The surface SHG experiments described in this Letter solely measure the transient changes in the surface electrostatic fields brought about by changes in the concentration of photogenerated holes at the electrode surface and do not distinguish between the consumption of photogenerated holes via interfacial charge transfer, surface recombination by charge trapping, or surface recombination by electron diffusion into the illuminated spot. However, the 3−4 ns time scale observed in the SHG experiments agrees with the time scales for these processes reported previously by the other optical methods.

The transient drop in SHG intensity due to the finite time required for the photogenerated holes to move to the surface of the TiO_2 electrode is shown with higher time resolution in Figure 3. The drop in SHG intensity as a function of pulse separation time can be fit with an exponential decay yielding a decay time constant, τ, of 36 ps for the particular surface region sampled in the experiment. The value of τ varied from spot to spot due to the inhomogeneity of the surface. Figure 4 displays a number of τ values obtained from different positions on the surface for three different pH solutions as a function of the total band bending (ΔV_{sc}). No systematic variation in τ was observed with changes in either pH or ΔV_{sc}. Additionally, τ did not show any dependence on the addition of phosphate (a surface blocking anion)[25,38] or sulfite (a hole-scavenging anion).[25,39] The average hole transit time for all of the measurements plotted in Figure 4 was 25 ps with a standard deviation of 8 ps.

This average hole transit time can be used to estimate the average surface hole drift velocity, ν_h, for this n-TiO_2 electrode. If we assume that the average distance traversed by the photogenerated holes is roughly 10 nm, a τ of 25 ps implies a value of 4×10^4 cm s^{-1} for ν_h. At low electrostatic fields, the hole drift velocity is linearly related to E_{dc} by the hole mobility,

μ_h ($\nu_h = \mu_h E_{dc}$).[40] Using a value of 4×10^4 cm s^{-1} for ν_h and a surface dc electric field of 2.5 kV cm^{-1} for this n-TiO_2 electrode as obtained from eq 2, a hole mobility, μ_h, of 16 cm^2 V^{-1} s^{-1} can be calculated for photogenerated holes in the first 20 nm of the space charge layer near the surface. This "near-surface" μ_h is approximately 30 times greater than the bulk μ_h obtained from the literature value for the hole diffusion constant ($D = 1.34 \times 10^{-2}$ cm^2 s^{-1})[6] via the Einstein relationship ($\mu_h = De/kT$).[40] There are two possible reasons for this variation: first, it is likely that, for the high electric fields and short length scales used in these transient band flattening experiments, the drift velocity is not linearly related to the bulk hole mobility, diffusion constant, or dc electric field.[36,40] Deviations from this direct relationship of ν_h and E_{dc} have been observed in GaAs at electrostatic fields above 3 kV cm^{-1} [36] and in Si above 10 kV cm^{-1}.[41] A second possible reason for the variation in μ_h is that the dc electric fields calculated from eq 2 may be too small. Variations in the magnitude of the actual surface electrostatic fields from those obtained by eq 2 are possible if either (a) the TiO_2 crystal had a higher doping density in the near surface region than in the bulk[31] or (b) a more exact, numerical solution of Poisson's equation was used to calculate the dc electric fields at the surface.[29]

A second important result, as shown in Figure 4, is that the hole drift velocity, ν_h, was independent of the electric field strength within the error limits of our measurements. It is possible that, at the high electric fields present at the TiO_2 surface, the holes have reached their saturation drift velocity.[40] To the best of our knowledge, no value for the saturation drift velocity for TiO_2 has been reported previously in the literature. On the other hand, τ is not expected to vary greatly over the wide range of band bending displayed in Figure 4 because the changes in the dc electric fields expected as a function of potential are actually quite small. Although ΔV_{sc} varies from 0.4 to 1.4 V in Figure 4, the time constant τ should depend on $\Delta V'_{sc}$, which is the steady-stae band bending under UV illumination. Using the steady-state measurements shown in Figure 1, a change in $\Delta V'_{sc}$ of only 0.15 V is expected for a change in ΔV_{sc} from 0.4 to 1.4 V. This implies that E_{dc} at the electrode surface as calculated from eq 2 only varies from 1.7 to 2.5 kV cm^{-1}. This variation in E_{dc} is not substantial enough to result in any changes in τ outside the standard deviation of ± 8 ps observed in our experiments. A systematic series of experiments on n-TiO_2 electrodes at different doping densities is required to fully discern the relationship between ν_h and E_{dc} in this near surface region.

In summary, the surface EFISH response of the n-TiO_2 semiconductor electrode/electrolyte interface has been used to obtain direct measurements of the surface dc electrostatic fields on picosecond and nanosecond time scales during the process of band flattening by UV excitation. Through a series of pump−probe transient band-flattening experiments, an average transit time of 25 ps is observed for the movement of photogenerated holes to the interface from the first 20 nm of the TiO_2 electrode surface. This average transit time does not vary significantly with band bending, pH, or solution composition. These experiments are the first time-resolved SHG measurements of the electrostatic fields at a semiconductor/electrolyte interface and demonstrate the utility of this technique as a probe of ultrafast phenomena at semiconductor electrodes. From the average transit time an average surface hole drift velocity of 4×10^4 cm s^{-1} is estimated; this value differs from that expected from the reported values for the bulk hole mobility. A time scale of 3−4 ns is observed for the removal of the excess photogenerated holes at the electrode surface by a combination of electrochemical charge transfer and surface recombination processes. Future experiments will focus on the dependence of the transient band flattening on doping density and surface morphology.

Acknowledgment. The authors gratefully acknowledge the support of the National Science Foundation in these studies. They also thank Prof. R. J. Hamers and Prof. K. Uosaki for helpful discussions.

References and Notes

(1) Lewis, N. S. *Annu. Rev. Phys. Chem.* **1991**, *42*, 543.
(2) Koval, C.; Howard, J. *Chem. Rev.* **1992**, *92*, 411.
(3) Nozik, A. J. *Annu. Rev. Phys. Chem.* **1978**, *29*, 189.
(4) *Energy Resources through Photochemistry and Catalysis*; Grätzel, M., Ed.; Academic Press: New York, 1983.
(5) Fox, M. A.; Dulay, M. T. *Chem. Rev.* **1993**, *93*, 341.
(6) Nakabayashi, S.; Komuro, S.; Aoyagi, Y.; Kira, A. *J. Phys. Chem.* **1987**, *91*, 1696.
(7) Kasinski, J. J.; Gomez-Jahn, L. A.; Faran, K. J.; Gracewski, S. M.; Miller, R. J. D. *J. Chem. Phys.* **1989**, *90*, 1253.
(8) Lu, H.; Prieskorn, J. N.; Hupp, J. T. *J. Am. Chem. Soc.* **1993**, *115*, 4927.
(9) Kay, A.; Humphry-Baker, R.; Grätzel, M. *J. Phys. Chem.* **1994**, *98*, 952.
(10) Kenyon, C. N.; Ryba, G. N.; Lewis, N. S. *J. Phys. Chem.* **1993**, *97*, 12928.
(11) Ryba, G. N.; Kenyon, C. N.; Lewis, N. S. *J. Phys. Chem.* **1993**, *97*, 13814.
(12) Rosenwaks, Y.; Thacker, B. R.; Nozik, A. J.; Ellingson, R. J.; Burr, K. C.; Tang, C. L. *J. Phys. Chem.* **1994**, *98*, 2739.
(13) Dekorsy, T.; Pfeifer, T.; Kütt, W.; Kurz, H. *Phys. Rev. B* **1993**, *47*, 3842.
(14) Rosetti, R.; Brus, L. E. *J. Phys. Chem.* **1986**, *90*, 558.
(15) Zhang, J. Z.; O'Neil, R. H.; Roberti, T. W. *J. Phys. Chem.* **1994**, *98*, 3859.
(16) Corn, R. M.; Higgins, D. A. *Chem. Rev.* **1994**, *94*, 107.
(17) Richmond, G. L. In *Electroanalytical Chemistry*; Bard, A. J., Ed.; Marcel Dekker: New York, 1991; Vol. 17, p 87.
(18) Shen, Y. R. *The Principles of Nonlinear Optics*; Wiley: New York, 1984.
(19) Heinz, T. F. In *Nonlinear Surface Electromagnetic Phenomena*; Ponath, H. E., Stegeman, G. I., Eds.; North-Holland: Amsterdam, 1991.
(20) Eisenthal, K. B. *Annu. Rev. Phys. Chem.* **1992**, *43*, 627.
(21) Lantz, J. M.; Baba, R.; Corn, R. M. *J. Phys. Chem.* **1993**, *97*, 7392.
(22) Kautek, W.; Sorg, N.; Kruger, J. In *Semiconductor Processing and Characterization with Lasers—Applications in Photovoltaics*; Trans Tech Publications Ltd.: Aedermannsdorf, Switzerland, in press.
(23) Fischer, P. R.; Daschbach, J. L.; Richmond, G. L. *Chem. Phys. Lett.* **1994**, *218*, 200.
(24) Qi, J.; Yeganeh, M. S.; Koltover, I.; Yodh, A. G.; Theis, W. W. *Phys. Rev. Lett.* **1993**, *71*, 633.
(25) Lantz, J. M.; Corn, R. M.; *J. Phys. Chem.* **1994**, *98*, 4899.
(26) Campbell, D. J.; Higgins, D. A.; Corn, R. M. *J. Phys. Chem.* **1990**, *94*, 3681.
(27) Lantz, J. M. Thesis, University of Wisconsin—Madison, 1994.
(28) Uosaki, K.; Kita, H. *J. Electrochem. Soc.* **1983**, *130*, 895.
(29) Rhoderick, E. H.; Williams, R. H. *Metal-Semiconductor Contacts*; Clarendon Press: Oxford, 1988.
(30) Uosaki, K.; Kita, H. In *Modern Aspects of Electrochemistry, No. 18*; White, R. E., Bockris, J. O., Conway, B. E., Eds.; Plenum Publishing: 1986; Vol. 18.
(31) Finklea, H. O. *Semiconductor Electrodes*; Elsevier: Amsterdam, 1988.
(32) Lee, C. H.; Chang, R. K.; Bloembergen, N. *Phys. Rev. Lett.* **1967**, *18*, 167.
(33) Guyot-Sionnest, P.; Tadjeddine, A. *J. Chem. Phys.* **1990**, *92*, 734.
(34) Ong, S.; Zhao, X.; Eisenthal, K. B. *Chem. Phys. Lett.* **1992**, *191*, 327.
(35) Corn, R. M.; Romagnoli, M.; Levenson, M. D.; Philpott, M. R. *Chem. Phys. Lett.* **1984**, *106*, 30.
(36) Chang, C. S.; Fetterman, H. R. *Solid-State Electron.* **1986**, *29*, 1295.
(37) Williams, F.; Nozik, A. J. *Nature* **1978**, *271*, 137.
(38) Noufi, R. N.; Kohl, P. A.; Frank, S. N.; Bard, A. J. *J. Electrochem. Soc.* **1978**, *125*, 246.
(39) Dutoit, E. C.; Cardon, F.; Gomes, W. P. *Ber. Bunsen-Ges. Phys. Chem.* **1976**, *80*, 1285.
(40) Sze, S. M. *Physics of Semiconductor Devices*; John Wiley & Sons: New York, 1981.
(41) Modelli, A.; Manzini, S. *Solid-State Electron.* **1988** *31*, 99.